The relationships between extreme winter North Atlantic extratropical cyclone hazards and modes of seasonal climate variability

Amanda C. Maycock[1,*], Christine M. McKenna[1,2], Matthew D. K. Priestley[3], Jacob Perez[4], Zhuo Li[1,5], Julia F. Lockwood[6]

[1] Institute for Climate and Atmospheric Science, School of Earth and Environment, University of Leeds, Leeds, UK

[2] JBA Consulting, Warrington, UK

[3] Department of Mathematics and Statistics, University of Exeter, Exeter, UK

[4] Centre for Doctoral Training in Fluid Dynamics, School of Computing, University of Leeds, Leeds, UK

[5] School of Atmospheric Sciences, Nanjing University, Nanjing, China

[6] Met Office Hadley Centre, Exeter, UK

Correspondence to: Amanda C. Maycock (a.c.maycock@leeds.ac.uk)

Abstract. North Atlantic extratropical cyclones (ETCs) cause significant financial losses in Europe, particularly in winter. Previous work has shown seasonal relationships between ETC hazards and modes of North Atlantic atmospheric variability, including the North Atlantic Oscillation (NAO; PC1) and East Atlantic Pattern (EAP; PC2). This study examines the relationship between the most extreme ETC hazards experienced at a given location in a winter season with the NAO and EAP, focusing on the winter maximum 10 metre wind gust and coastal significant wave height, and the daily maximum and winter total precipitation. We examine compound effects where PC1 or PC2 have signals in multiple hazard types at the same location. Positive PC1 exhibits coincident increases in winter maximum wind gust and significant wave height hazards around most coastal regions in northern Europe. Positive PC2 exhibits coincident increases in winter maximum wind gust and daily precipitation hazards over land areas in southern UK, Portugal and Spain, with an additional compound effect from increased significant wave height near southern UK, northern France and Spain coasts. We also consider compound effects where PC1 and PC2 show coincident signals in the same hazard at a given location, potentially indicating an elevated hazard likelihood when circulation anomalies project onto both modes concurrently. PC1 and PC2 have coincident signals for wind gusts in southern Ireland, southern UK, Portugal and Scandinavian coast. For significant wave height, PC1 and PC2 have coincident signals around the Scandinavian, southern UK and Ireland and Northern Portugal coasts. This study shows that large-scale modes of seasonal North Atlantic climate variability modulate the exposure to extreme ETC hazards in many parts of Europe. The results have the potential to be combined with skilful seasonal climate forecasts of PC1 and PC2 to inform the insurance sector.

1 Introduction

North Atlantic extratropical cyclones (ETC) are the primary source of winter-time weather related hazards in Europe, including damaging winds, heavy precipitation and marine wave swell. These hazards have caused billions of Euros of damages in affected seasons (e.g., Moemken et al., 2024), particularly in boreal winter when the North Atlantic storm track is most active. Seasonal climate forecasts aim to predict the risk of weather and climate hazards several months in advance, so that preparatory action can be taken to mitigate anticipated impacts. One source of potential predictability on seasonal-to-annual timescales is via the relationship of ETC hazards with large-scale modes of atmospheric variability, which can be predictable on seasonal timescales. In particular, seasonal forecast models have shown predictive skill for the winter North Atlantic Oscillation (NAO, e.g., Scaife et al., 2014) and the early winter East Atlantic pattern (EAP, Thornton et al., 2023), so these modes are the focus of this study. If a mode of variability can be skilfully predicted, then information about the exposure to ETC hazards can be deduced (e.g., Befort et al., 2019; Degenhardt et al., 2023, 2024; Lockwood et al., 2023). It is therefore of value to derive observed relationships between ETC hazards and modes of variability, to inform the assessment of potential sources of predictive skill.

Previous work has shown that winter storm characteristics (Pinto et al., 2009) including the pattern of winter wind gusts (e.g., Donat et al., 2010; Befort et al., 2019; Degenhardt et al., 2023, 2024; Lockwood et al., 2023) and wave swell (e.g., Bacon & Carter, 1993; Dodet et al., 2010; Izaguirre et al., 2010, 2011; Martinez-Asensio et al., 2016; Castelle et al., 2018) in northern Europe are correlated with the NAO. Furthermore, when the NAO is in a positive phase there are generally wetter winter conditions in the UK and northern Europe and drier conditions in southern Europe (Hurrell et al., 2003). A positive EAP phase is associated with an increase in cumulative winter storm severity in the UK, though for an equivalent change in index the amplitude of the storm severity signal is weaker than for the NAO (Degenhardt et al., 2023), but there is relatively little signal of the EAP in storm severity in continental Europe. Many existing studies consider seasonal hazards and do not explicitly consider short timescale extremes, which are often linked to considerable impacts. Furthermore, there has been less attention paid to the relationship of North Atlantic modes of variability with compound hazards, where a particular region or location may experience more than one extreme hazard within a season (e.g., heavy precipitation and strong winds; Matthews et al., 2014, Hillier et al., 2015, Martius et al., 2016). Such compound events can increase overall damages, leading to higher insurance claims and longer timescales to restore infrastructure following the events (Hillier et al., 2015, 2025; Bloomfield et al., 2023). Therefore, there is value in quantifying the relationships of compound hazards with modes of variability for the purposes of understanding potential seasonal predictability.

This study addresses the following questions:

1) How are the two leading modes of North Atlantic atmospheric variability – the NAO and EAP – related to spatial variability in extreme ETC hazards due to wind gusts, daily precipitation rates and significant wave height?
2) In which regions do the NAO and EAP induce more than one ETC hazard (compound hazards) and in which regions do the two modes have geographically overlapping hazard signals (i.e. both modes contribute to the local risk)?

We note that a similar analysis could be performed without restricting the hazards to those occurring within ETCs. However, the linkage with ETCs provides a robust physical connection, since the large-scale modes of variability are associated with variations in the North Atlantic eddy-driven jet speed and position, which in turn shape the baroclinic environment that controls the formation of ETCs. It is also widely known that the most severe winter weather hazards in Europe are associated with ETCs. The focus on ETC related meteorological hazards therefore provides a useful physical lens to interpret the influence of the modes of large-scale variability. The remainder of the paper is structured as follows: Section 2 describes the datasets used in the study and the analysis methods; Section 3 describes the Results and Section 4 summarises our main conclusions.

2 Methods

2.1 Datasets

The analysis uses ERA5 reanalysis data based on the Integrated Forecasting System (IFS) Cycle 41r2 (Hersbach et al., 2020). Data are extracted for the entire calendar year from 1980-2020 and 40 complete winters (Dec-Feb) are analysed labelled by the year of Jan-Feb (i.e. 1981-2020). The variables used in the analysis are 850 hPa relative vorticity (variable 'vo'), mean sea level pressure (variable 'msl'), maximum 10 metre wind gust since previous preprocessing (variable '10fg'), total precipitation (variable 'pr'), and significant height of combined wind waves and swell (variable 'swh', hereafter significant wave height). ERA5 is provided at a 0.25x0.25 degree resolution (0.5x0.5 degrees for 'swh' variable) and used at 1 hourly temporal frequency.

Winter average near-surface wind speeds in Europe in ERA5 have been shown to agree better with observation towers than several other reanalysis datasets (Ramon et al., 2019). As is standard for climate models, wind gusts are post-processed in ERA5 following the approach described in ECMWF (2016). Comparison with meteorological station data in Sweden indicates strong wind gusts (>~15 m/s) are generally underestimated in ERA5 (Minola et al., 2020). This is consistent with Chen et al. (2024), who evaluated ERA5 against weather station observations in North America and showed that in DJF spatially-averaged near-surface wind speeds within ETCs are well represented (r ~0.9), but wind speeds associated with the most intense ETCs and local extremes within ETCs are generally underestimated. Lodise et al. (2024; their Fig 7) also compared Northern

hemisphere ETC wind speeds in ERA5 with radar altimeter measurements and found ERA5 has a low bias by ~5% in the region of strongest 10m wind speeds on the eastern hemisphere of the cyclone relative to the translational direction. For significant wave height, Bessonova et al. (2025) and Fanti et al. (2023) compared ERA5 to global buoy measurements and found an underestimation in ERA5 which was most pronounced for larger wave height measurements. Lodise et al. (2024) also found that in ERA5 significant wave heights within Northern hemisphere ETC footprints are biased low by ~5% compared with radar altimeter data. For daily precipitation, ERA5 shows the smallest biases in the winter extratropics compared to other global regions and seasons (Lavers et al., 2022) and captures observed variability across Europe with significant skill compared with E-OBS observations (Bandhauer et al., 2021). However, ERA5 underestimates the magnitude of extreme daily precipitation but it can generally capture the location and timing of precipitation extremes (Lavers et al., 2022). Therefore, based on studies that have evaluated ERA5, we conclude that the extreme European ETC hazards derived in this study are likely to be conservative estimates.

2.2 ETC tracking

The TRACK algorithm is used to identify and track ETCs (Hodges, 1994, 1995, 1999). TRACK identifies ETCs based on maxima in the hourly 850 hPa relative vorticity field. Prior to tracking, the vorticity field is spectrally truncated to T42 resolution and filtered to remove wavenumbers less than 5, which ensures the analysis focuses on synoptic scale disturbances. Following identification of cyclonic maxima, identification points are refined using a B-spline interpolation and steepest ascent maximization. ETCs are then grouped into tracks using a nearest neighbor approach. These are then refined by the minimization of a cost function for track smoothness subject to adaptive constraints. As we are only interested in well-developed and long-lived ETCs, tracks must persist for at least 48 hours and travel at least 1000 km from their origin. Due to the focus of this study being on Europe and the North Atlantic, only tracks that are present in the region 30-75°N, 260-40°E are retained in the analysis. For each track in the study region, we identify the atmospheric and oceanic state that is attributable to the presence of the ETC based on a distance criterion. At each hourly step in the lifecycle, the hazard 'footprint' around the ETC is extracted using a radial distance of either 5° or 10° from the cyclone centre. A 5° radius is used for the wind gust and significant wave height variables and a 10° radius for precipitation. This is due to the maximum winds of an ETC mainly being within 5° of the cyclone centre (Priestley and Catto, 2022), but a larger area of influence on precipitation due to the scale of fronts (Kodama et al., 2019). The analysis focuses on the boreal winter season from December-February (DJF) when the North Atlantic storm track is most active, so the ETC tracks are filtered to retain DJF storms.

2.3 ETC hazard footprints

The ETC hazard variables examined are the maximum daily precipitation or equivalently the wettest winter day due to an ETC, the winter total precipitation due to ETCs, the maximum 3 second 10m wind gust, and the maximum significant wave

height. The first measure relates to the likelihood of flooding, particularly pluvial flooding in urban areas or fluvial flooding in catchments with high antecedent soil moisture (e.g., Ivancic et al., 2015); it is similar to the commonly used Rx1day metric which represents the wettest calendar day in the year and is widely used in the climate extremes literature (e.g., Seneviratne et al., 2021). The second metric represents the cumulative winter precipitation due to ETCs which is also related to flood hazards due to the relationship with antecedent moisture (e.g., Bennett et al., 2018). The third hazard measure relates to the likelihood of wind damage; and the third relates to the likelihood of coastal flooding from wave overtopping. The hazard footprints resulting from the tracking (Section 2.1) are post-processed to extract the maximum value at each gridpoint the ETC intersects over its lifecycle, or in the case of precipitation the maximum daily accumulation and the total accumulation over the ETC lifecycle. The choice of analysing the most extreme hazards within the season provides an upper limit on the most hazardous conditions that might be expected based on a relationship with the seasonal modes of variability; this extends previous work that has taken a seasonally aggregate view (e.g., Degenhardt et al., 2023) and may be useful to stress test the resilience of infrastructure and buildings to extreme hazards. An example of the hazard footprints identified from this method for Storm Ciara in February 2020 is shown in Figure 1.

For each winter season, the hazard footprints from all tracked ETCs are overlaid and the maximum value at each gridpoint is then selected for the winter. The resulting field therefore represents the most extreme ETC hazard (maximum 3 second 10m wind gust, maximum hourly significant wave height, or daily precipitation) experienced at each gridpoint in a given winter; these are used in the regression analysis. This approach is distinct from the seasonal average or cumulative perspective that has been used in some other studies and emphasises short-term extreme hazards. Note, the extremes are therefore not spatially contiguous and the values at neighbouring gridpoints may come from different ETCs within a given season.

For part of the analysis, we also calculate a storm damage index (SDI) (Karremann et al. 2014), which is the population weighted meteorological storm severity index (SSI) (Klawa and Ulbrich 2003). The SSI is calculated as

$$SSI_{i,j} = \left(\frac{v_{i,j}^{max}}{v_{i,j}^{98}} - 1\right)^3, \qquad \text{(Equation 1)}$$

where i and j are the gridbox coordinates, v_{max} is the maximum wind speed value associated with the ETC, v_{98} is the 98th percentile of the winter wind speed distribution over December 1980 - February 2020. Negative values of SSI are set to zero to ensure cyclonic wind speeds below the 98th percentile threshold do not contribute to the loss metrics.

Since the losses associated with windstorms will be strongly related to the exposure of people and buildings, the SSI can be scaled by the population estimate at each grid box to estimate a storm damage index (SDI)

$$SDI_{i,j} = SSI_{i,j} \times population_{i,j}, \qquad \text{(Equation 2)}$$

where gridded population data for 2015 are taken from the Gridded Population of the World fourth version (GPWv4; doi:10.7927/H49C6VHW). For comparison with earlier studies, the SDI is summed over all storms within a given season to give a seasonal SDI value (e.g., Degenhardt et al., 2023).

2.4 North Atlantic modes of variability

The NAO and EAP (also known as the Atlantic Ridge) modes of variability are calculated as the first two empirical orthogonal functions (EOF1 and EOF2) of DJF mean sea level pressure in the Euro-Atlantic sector (90°W-40°E, 20-80°N following Hurrell (1995)) and the associated principal component timeseries (PC1 and PC2). These are hereafter referred to as PC1 and PC2, respectively.

2.5 Regional analysis

The ETC hazards are assessed quantitatively for land and sea subregions within the analysis domain (25°W-40°E; 35-75°N). Land regions are defined following the 0.5 Mm^2 regions of Stone (2019), which represent approximately equal areas regions along political/economic boundaries and have been previously used to study climate extreme hazards. There are The regional seas are defined following the European Environment Agency regions defined by the EU (https://sdi.eea.europa.eu/data/51035cd2-3dea-4b39-94c7-e53946603c2a), these categorise four main European seas: Mediterranean, Baltic, Black Seas and North East Atlantic Ocean, all of which except the Baltic Sea are further divided into subregions. There are 16 land regions and 15 regional sea regions analysed in the study. The hazards are first averaged over the regions before being analysed for their covariance with the NAO and EAP.

2.6 Regression analysis

We perform least squares linear and multiple linear regression of the winter maximum ETC hazards at each gridpoint against the winter mean PC1 and PC2 timeseries within the Euro-Atlantic domain 25°W-40°E, 35-75°N. To assess the suitability of the statistical model to describe the data, we examine the R^2, linearity, metric homoscedasticity, normality of residuals and the independence using the Durbin Watson (DW) statistic to test for autocorrelation in the residuals. The DW statistic ranges from 0 to 4, with a value of 2 indicating zero autocorrelation in the residuals. For linearity, homoscedasticity and normality we assess p-values using a 95% confidence level, such that $p<0.05$ denotes the required condition is not met and the regression model performance is unsatisfactory, while $p>0.05$ denotes the condition is met.

Some previous studies have investigated the signals of North Atlantic modes of variability in seasonal European SDI and ETC frequency based measures (e.g., Degenhardt et al., 2023). We also tested our analysis on these variables but found issues with the performance of linear regression at the grid point scale.

By construction, SDI = 0 when $v_{max}<v_{98}$ (see Equation 1). This non-linear behaviour means a linear regression is likely to perform poorly if applied over all time points. Typical performance of linear regression for SDI against PC1 and PC2 is shown in Figure 2 for a gridpoint near Birmingham (52.5°N, 2.0°W). Figure S1 shows the full statistical metrics for the linear regression performance for SDI across our study region. While statistically significant regression coefficients against PC1 and PC2 are obtained in some regions (Figure S1a, cf. Degenhardt et al., 2023), the analysis of the regression performance reveals the homoskedasticity and normality criteria are poorly met within those regions (Figure S1c), meaning there is too much variance and non-normal behaviour in the error term and the model isn't well defined. Therefore, while reasonable total R^2 values can in principle be achieved (Figure S1b), the linear model is not suitable for this data. Hence, we do not perform further analysis of SDI in this study. Previous studies have generally presented R^2 values for similar regression analyses but not further measures of model performance.

ETC frequency related measures, such as total count or number of ETCs exceeding a specified wind gust threshold, are discrete variables where linear regression can perform poorly. Fewer issues were found with the performance of linear regression for seasonal ETC count (Figure S2), though some European regions show residuals that do not satisfy the criteria of normality or zero autocorrelation in the residuals. Therefore, we encourage caution in applying simple statistical analyses like linear regression to data which may not satisfy the requirements for a linear model. For these reasons we do not include frequency and SDI based ETC hazard metrics in this study.

3. Results

3.1 Signatures of NAO and EAP in ETC hazards

Figure 3 shows the climatological winter maxima derived from the cyclone footprints and PC1 and PC2 regression maps for the four ETC hazard types: (a) winter total precipitation, (b) maximum daily precipitation accumulation, (c) winter maximum 10m wind gust and (d) winter maximum significant wave height. The PC1 and PC2 regression slopes are shown as percentage anomalies from the climatology, with equivalent absolute anomalies shown in Figure S3. The accompanying R^2 values for the regressions are shown in Figure 4 and the evaluation of the regression performance is shown in Figure S4, which shows the linear regression performs much better for these variables than those discussed in Section 2.4.

The relationship between PC1 and winter total precipitation in Europe due to ETCs is similar to that found for precipitation not conditioned on ETCs (e.g., McKenna and Maycock, 2022), with wetting over the UK and Scandinavia and drying over the Iberian peninsula (Fig. 3aii), consistent with the majority of winter European precipitation falling within ETCs (Hawcroft et al., 2012). For PC2, the signal comprises an increase in winter precipitation over the UK, western France and the Iberian peninsula with drying over Scandinavia (Fig. 3aiii). In contrast to the coherent signals in winter total precipitation from ETCs

with PC1, there is a much weaker relationship with the winter maximum daily precipitation from ETCs, though where a significant relationship is seen, the canonical NAO north/south Europe wet/dry dipole pattern is evident (Fig. 3bii). In contrast, a positive PC2 anomaly corresponds with a significant increase in winter maximum daily precipitation over Portugal and parts of western UK (Fig. 3biii). Scaife et al. (2008) showed a relationship between 5-day precipitation extremes and the NAO, with more events above the 90th percentile and less events below the 10th percentile over the UK and northern Europe during NAO positive. The lack of significant relationship with PC1 could be a result of the relatively noisy data, since at each gridpoint we are taking the wettest day in the winter associated with any ETC and regressing this against the seasonal NAO.

In contrast, there is a strong signal of winter maximum 10m wind gust in both PC1 and PC2, with large regions with anomalies of 10-15% above climatology (Fig. 3c). For positive PC1, the UK, Scandinavia, Netherlands and Northern Germany show increased maximum wind gusts, while Portugal and Northern Spain show a decrease (Fig. 3cii). For positive PC2, southern and south-west England and Wales show an increase wind gust along with Portugal and Spain, while parts of Scandinavia and eastern Mediterranean show a reduction (Fig. 3ciii).

The patterns of anomalous significant wave height largely mirror those of wind gusts, reflecting their known relationship (e.g., Dobrynin et al., 2019), with positive height anomalies of 10-15% around the UK and Scandinavian coasts for PC1 (Fig. 3dii). For PC2, there are comparable anomalies around Southern Ireland and south-west England, as well as anomalies of 5-10% around the French, Portuguese and Spanish coastlines (Fig. 3diii).

In regions where the regression coefficients are statistically significant, the combined PC1 and PC2 regressions explain up to around 50% of the interannual variance of the winter maximum wind gust and significant wave height, and locally up to around 70% for winter total precipitation due to ETCs but less for winter maximum daily precipitation over land areas (Figure 4).

3.2 Regional average hazards for PC1/PC2

Figure 5 shows percent anomalies in winter total precipitation, winter maximum wind gust and significant wave height due to ETCs associated with a +1σ anomaly of PC1 and PC2 aggregated to regional scales over land and ocean areas. At regional scales, the proportionately largest signals for PC1 (Fig. 5a) are in precipitation including increases of 8.9% in West Russia, 17.5% in North-West Russia, 15.9% in Finland and Baltic Seas, 12.0% in Sweden and 16.2% in the UK, Denmark and Norway. There are also significant increases in wind gusts in these regions with a smaller relative magnitude of <10%. There are significant anti-correlations between the hazards and PC1 in southern Europe including a decrease of 34.4% in the Iberian Peninsula, -10.2% in France, 13.5% in Italy and 14.7% in Romania, Bulgaria and Greece; however, there are no significant anomalies in maximum wind gust in these regions except for the Iberian Peninsula (-7.7%). As expected, over ocean regions

the anomalous wind gusts and significant wave height have similar magnitudes typically 5-10% over exposed seas in the western part of the domain (Celtic Seas, Macaronesia, Iceland Sea, Greater North Sea, Norwegian Sea and the Baltic Sea.

For PC2 (Fig. 5b), the significant precipitation and wind gust signals are generally weaker over continental Europe, except for the Iberian peninsula (Pr = 26.4%, G=10.5%), France (Pr = 13.0%) and Sweden (G = -6.0%). There are significant collocated wind gust and significant wave height anomalies with PC2 over western and northern seas: Macaronesia, Bay of Biscay and Iberian Sea, Norwegian Sea and Barents Sea.

3.3 Compound multivariate hazards for PC1/PC2

Compound events where multiple hazards coincide in space and time are often particularly impactful (e.g., Owen et al., 2021). The results in Figures 3 and 5 show areas of considerable overlap between the individual ETC hazards. To determine all the locations where either PC1 or PC2 modify one ETC hazard, we overlay the coloured areas for the winter total precipitation, wind gust and significant wave height hazard regression maps from Figure 3 and plot the geographical coverage distinguishing regions affected by a single hazard types, regions unaffected by any hazard and regions affected by >1 hazard (Fig. 6a). An equivalent analysis for multivariate hazards where there are coincident signals in multiple variables for either PC1 or PC2 is performed; these are shown for permutations of two hazard types and all three hazards in Fig 6b. Note given these are statistical relationships, we are not establishing whether the extremes occur from the same ETC and are therefore coincident in time; rather, this reflects whether regions could experience enhanced exposure to multivariate hazards within a winter season, depending on the relative phases of PC1 and PC2.

PC1 alters the exposure to only cumulative winter precipitation in Spain, southern France and northern Norway, Sweden and Finland. PC1 alters the intensity of only peak wind gusts in eastern England, the Netherlands, northern Germany, central Norway and Sweden and Baltic countries. PC1 does not affect hazard exposure in France, Switzerland, Germany and most countries in central and eastern Europe. For compound hazards, PC1 mainly associates with altered exposure to paired winter precipitation and wind gust hazards in Ireland and the western UK, western Norway, southern Sweden, Finland and western Russia. Compound wind gust and significant wave height hazards occur in the Irish Sea, the Channel, North Sea and Baltic Sea. The areas with compound exposure to all three hazards for PC1 are in the Atlantic Ocean, Norwegian Sea and parts of the Iberian Sea.

For PC2, there is no discernible change in exposure to any single hazard across most of central and eastern Europe (Fig. 6b). Central and northern England, Scotland, Ireland, northern and western France and western Norway show only altered exposure to winter precipitation amount for PC2. For compound hazards, PC2 alters exposure to winter precipitation and peak wind gust

for Portugal and western Spain. PC2 alters exposure to wind gust and significant wave height in the eastern Mediterranean and around the coast of Norway. The coasts around southern Ireland, Wales, south-west England, northern France and Portugal show altered exposure to all three hazards for PC2 which operate in the same sign (i.e. wetter, windier and higher significant wave height for positive PC2).

300

3.3 Compound hazards for combined PC1/PC2 circulation

Many winters show anomalous North Atlantic atmospheric circulation that partly projects onto both PC1 and PC2, so it is possible that at some locations the exposure to ETC hazards will be modulated by both modes of variability. To determine
305 these regions for each hazard type, we follow a similar process to Section 3.2 where the coloured areas from the regression maps in the middle and right columns of Fig. 3 are overlaid along each row. Where the two fields coincide shows the locations where the exposure to the hazard type will be affected by both PC1 and PC2. The resultant locations are shown in Figure 7 for the winter total precipitation, wind gust and significant wave height. Figure 7 reveals virtually no regions of compound maximum daily precipitation hazards over land, but coherent regions where PC1 and PC2 affect variability for wind gusts and
310 significant wave height. These regions are Portugal, southern England, Wales, southern Ireland, southern Scandinavia. As before, over ocean points the patterns for the two variables are similar given that significant wave height is strongly driven by near-surface wind. The overlapping patterns for these variables indicates the absolute change in exposure to ETC hazards in a given winter will be affected by the relative amplitudes of PC1 and PC2.

315 To further illustrate this, Figure 8 shows absolute values of the expected ETC hazards for unitary combinations of the standardised PC1 and PC2 indices (i.e. +1σ PC1 and +1σ PC2; +1σ PC1 and -1σ PC2, etc., as shown by red dots in middle panel Fig. 8). These are constructed by superposing the PC1 and PC2 signals onto the winter climatology over all years. The scatterplot in the centre of Figure 8 shows the combinations of PC1/PC2 indices in ERA5 for all winters from 1981-2020. Some combinations have been observed infrequently (PC1<0 and PC2<0), which shows it is rarely the case that negative NAO
320 occurs with Atlantic ridging, but all four combinations of indices used to present the hazards lie within the distribution of observed PC1/PC2 indices and are therefore plausible examples. The hazard maps include solid contours denoting specific thresholds for wind gusts, based on the Beaufort scale for severe gale (25 m/s), violent storm (29 m/s) and hurricane strength (33 m/s) gusts, and for significant wave height based on the Douglas Sea Scale, for very high (9m) and phenomenal (14m) heights.

325

For the combination PC1– and PC2+, the winter maximum wind gust reaches violent storm intensity along the west coast of Ireland and the Bay of Biscay and severe gale intensity along the Iberian peninsula and Norwegian coast (Fig. 8a). The maximum significant wave height reaches very high along the west coast of Ireland and precipitation is 10-30% above normal in southern Ireland, England and Iberia, with drier conditions in Scandinavia (Fig. 8a).

In comparison, for the combination of PC1+ and PC2+ the winter maximum wind gust reaches hurricane intensity along the west coast Ireland, in Wales, south-west England and Scotland, with severe gale intensity in south-east England (Fig. 8b). Maximum wind gust reaches violent storm intensity along the Norway, Sweden and Finland coastlines (Fig. 8b). The area where winter maximum significant wave height reaches very high levels is expanded compared to PC1- and PC2+, reaching south-west England and extending into the Norwegian Sea. Precipitation is 10-30% above normal in northern Scotland and the Iberian peninsula (Fig. 8b).

For PC1+ combined with PC2-, the area where winter maximum wind gust reaches hurricane intensity extends further east towards the Norwegian coast, with violent storm intensity near south-west England and Wales (Fig. 8c). In contrast, in southern Europe winter maximum wind gust is alleviated reaching less than severe gale force in the Iberian peninsula and severe gale force in the Bay of Biscay, Sweden and southern Finland. The region exposed to very high maximum significant wave height reaches the west of Ireland, Scotland, southern Iceland and the northern Norway coast (Fig. 8c). Precipitation shows drier than normal conditions in southern Ireland, England and Iberia, with above average precipitation in Scandinavia (Fig. 8c).

Lastly for PC1- combined with PC2-, winter maximum wind gust reaches severe gale intensity in the Bay of Biscay, with below severe gale level in southern England and Wales (Fig. 8d). Along the west coast of Ireland, northern Scotland and the Norwegian coast the maximum wind gust reaches violent storm intensity. The region exposed to very high significant wave height is more restricted to the west of Ireland. Maximum daily precipitation is 10-30% below normal in northern Scotland and Iberia (Fig. 8d).

These examples illustrate the importance of the signals of extreme ETC hazards associated with PC1 and PC2 variability for the exposure of different parts of Europe to the risk of severe weather events.

4. Discussion and conclusions

This study has investigated the relationships between extreme meteorological hazards in Europe associated with ETCs and the two leading modes of North Atlantic atmospheric variability: the North Atlantic Oscillation (PC1) and the East Atlantic pattern (PC2). ETCs were tracked and their footprints in key hazard variables - winter maximum 10m wind gust, maximum significant wave height, maximum daily precipitation and winter total precipitation - were extracted. The relationship of these variables with the seasonal winter NAO and EAP indices were derived using linear regression. To extend from earlier work (e.g., Befort et al., 2019; Degenhardt et al., 2023, 2024; Lockwood et al., 2023; Bloomfield et al., 2023), we focus on the most extreme event for a particular variable and location within a winter season and the year-to-year relationship of those extremes with large-scale modes of variability. The motivation for this is to understand the nature of the most extreme hazard that can be

expected to occur in a typical winter characterised by NAO and EAP circulation anomalies. Daily maximum precipitation and winter total precipitation are examined as both are relevant for flooding.

There are significant relationships of PC1 and PC2 with the ETC hazard variables in many regions of Europe. These overlap in some regions, indicating an interaction between modes of variability for the exposure in those regions to risks from weather hazards. The regressions for winter total precipitation are stronger and more statistically significant compared with the regressions for winter maximum daily precipitation because the latter hazard is inherently more variable and influenced by other factors than the large-scale North Atlantic circulation. We have further considered compound events where there may be increased exposure to multiple ETC hazards within a season. This was particularly the case for wind gust and significant wave height, which are physically coupled.

The analysis assumes the relationships of the strongest winter ETC hazards with the seasonal models of variability are well described by a linear model. While we have shown that some common ETC and hazard indices are not well suited to the application of linear regression at the grid point level, notably the storm damage index (SDI) and discrete variables like storm frequency, there also remains unexplained interannual variance for the other ETC hazards studied here. It would be valuable to explore these residuals in further work and to test other higher order statistical models or machine learning techniques which are suited to identifying non-linear relationships.

The findings of the study highlight the potential for predictive skill of large-scale modes on seasonal timescales (e.g., Scaife et al., 2014; Thornton et al., 2023) to be used to quantify the expected exposure to extreme winter ETC hazards in Europe. Since these events are regularly responsible for billions of euros of damages, this could provide information for stakeholders in the insurance, transport, energy and housing sectors.

References

Bacon, S. and Carter, D.J.T. (1993), A connection between mean wave height and atmospheric pressure gradient in the North Atlantic. Int. J. Climatol., 13: 423-436. https://doi.org/10.1002/joc.3370130406

Bandhauer, M., Isotta, F., Lakatos, M., Lussana, C., Båserud, L., Izsák, B., Szentes, O., Tveito, O. E., & Frei, C. (2022). Evaluation of daily precipitation analyses in E-OBS (v19.0e) and ERA5 by comparison to regional high-resolution datasets in European regions. *International Journal of Climatology*, 42(2), 727–747. https://doi.org/10.1002/joc.7269

Befort DJ, Wild S, Knight JR, *et al*. Seasonal forecast skill for extratropical cyclones and windstorms. *Q J R Meteorol Soc*. 2019; 145: 92–104. https://doi.org/10.1002/qj.3406

Bennett B, Leonard M, Deng Y, Westra S (2018) An empirical investigation into the effect of antecedent precipitation on flood volume. *J Hydrol* 567:435–445. https://doi.org/10.1016/j.jhydrol.2018.10.025

Bessonova, V., E. Tapoglou, R. Dorrell, N. Dethlefs and K. York (2025) Global evaluation of wave data reanalysis: Comparison of the ERA5 dataset to buoy observations, *Applied Ocean Research*, 157, 104490 https://doi.org/10.1016/j.apor.2025.104490

Bloomfield H, Hillier J, Griffin A, Kay A, Shaffrey L, Pianosi F, James R, Kumar D, Champion A and Bates P 2023 Co-occurring wintertime flooding and extreme wind over Europe, from daily to seasonal timescales *Weather Clim. Extremes* **39** 100550

Castelle, B., Dodet, G., Masselink, G., & Scott, T. (2018). Increased winter-mean wave height, variability, and periodicity in the northeast Atlantic over 1949–2017. *Geophysical Research Letters*, 45, 3586–3596. https://doi.org/10.1002/2017GL076884

Center for International Earth Science Information Network (CIESIN), Columbia University. 'Gridded Population of the World, Version 4 (GPWv4): Population Density, Revision 11.' Palisades, NY: Socioeconomic Data and Applications Center (SEDAC), 2017. doi:10.7927/H49C6VHW

Chen, T.-C., Collet, F., & Di Luca, A. (2024). Evaluation of ERA5 precipitation and 10-m wind speed associated with extratropical cyclones using station data over North America. International Journal of Climatology, 44(3), 729–747. https://doi.org/10.1002/joc.8339

Degenhardt, L., Leckebusch, G.C. & Scaife, A.A. Large-scale circulation patterns and their influence on European winter windstorm predictions. *Clim Dyn* **60**, 3597–3611 (2023). https://doi.org/10.1007/s00382-022-06455-2

Degenhardt, L., Leckebusch, G. C., and Scaife, A. A.: Understanding winter windstorm predictability over Europe, Weather Clim. Dynam., 5, 587–607, https://doi.org/10.5194/wcd-5-587-2024, 2024.

Dobrynin, M., Kleine, T., Düsterhus, A., & Baehr, J. (2019). Skilful seasonal prediction of ocean surface waves in the Atlantic Ocean. *Geophysical Research Letters*, 46, 1731–1739. https://doi.org/10.1029/2018GL081334

Dodet, G., X. Bertin, and R. Taborda, Wave climate variability in the North-East Atlantic over the last six decades, Ocean Model. **31**, 120–131 (2010).

Donat, M.G., Leckebusch, G.C., Pinto, J.G. and Ulbrich, U. (2010), Examination of wind storms over Central Europe with respect to circulation weather types and NAO phases. Int. J. Climatol., 30: 1289-1300. https://doi.org/10.1002/joc.1982

European Center for Medium-Range Weather Forecasts (ECMWF) (2016) IFS Documentation CY45R2—Part IV: Physical processes. IFS doc. https://www.ecmwf.int/node/16648. Accessed 8 May 2020

Fanti, V., Ferreira, Ó., Kümmerer, V. et al. Improved estimates of extreme wave conditions in coastal areas from calibrated global reanalyses. Commun Earth Environ 4, 151 (2023). https://doi.org/10.1038/s43247-023-00819-0

Hawcroft, M. K., L. C. Shaffrey, K. I. Hodges, and H. F. Dacre (2012), How much Northern Hemisphere precipitation is associated with extratropical cyclones?, *Geophys. Res. Lett*., 39, L24809, doi:10.1029/2012GL053866.

Hersbach H, Bell B, Berrisford P, et al. The ERA5 global reanalysis. Q J R Meteorol Soc. 2020; 146: 1999–2049. https://doi.org/10.1002/qj.3803

Hillier J K, Macdonald N, Leckebusch G C and Stavrinides A 2015 Interactions between apparently primary weather-driven hazards and their cost *Environ. Res. Lett.* **10** 104003

Hillier, J.K., Bloomfield, H.C., Manning, C., Garry, F., Shaffrey, L., Bates, P. and Kumar, D. (2025), Increasingly Seasonal Jet Stream Raises Risk of Co-Occurring Flooding and Extreme Wind in Great Britain. Int J Climatol e8763. https://doi.org/10.1002/joc.8763

Hodges, K. I.: A General Method for Tracking Analysis and Its Application to Meteorological Data, Mon. Weather Rev., 122, 2573–2586, https://doi.org/10.1175/1520-0493(1994)122<2573:AGMFTA>2.0.CO;2, 1994.

Hodges, K. I.: Feature Tracking on the Unit Sphere, Mon. Weather Rev., 123, 3458–3465, https://doi.org/10.1175/1520-0493(1995)123<3458:FTOTUS>2.0.CO;2, 1995.

Hodges, K. I.: Adaptive Constraints for Feature Tracking, Mon. Weather Rev., 127, 1362–1373, https://doi.org/10.1175/1520-0493(1999)127<1362:ACFFT>2.0.CO;2, 1999.

Hurrell, J.W., Kushnir, Y., Ottersen, G. and Visbeck, M. (2003). An Overview of the North Atlantic Oscillation. In The North Atlantic Oscillation: Climatic Significance and Environmental Impact (eds J.W. Hurrell, Y. Kushnir, G. Ottersen and M. Visbeck). https://doi.org/10.1029/134GM01

Ivancic, T.J., Shaw, S.B. Examining why trends in very heavy precipitation should not be mistaken for trends in very high river discharge. *Climatic Change* 133, 681–693 (2015). https://doi.org/10.1007/s10584-015-1476-1

Izaguirre, C., F. J. Mendez, M. Menendez, A. Luceño, and I. J. Losada (2010), Extreme wave climate variability in southern Europe using satellite data, *J. Geophys. Res.*, 115, C04009, doi:10.1029/2009JC005802.

Izaguirre, C., F. J. Méndez, M. Menéndez, and I. J. Losada (2011), Global extreme wave height variability based on satellite data, *Geophys. Res. Lett.*, 38, L10607, doi:10.1029/2011GL047302.

Karremann, M. K., Pinto, J. G., von Bomhard, P. J., and Klawa, M.: On the clustering of winter storm loss events over Germany, Nat. Hazards Earth Syst. Sci., 14, 2041–2052, https://doi.org/10.5194/nhess-14-2041-2014, 2014.

Klawa, M. and Ulbrich, U.: A model for the estimation of storm losses and the identification of severe winter storms in Germany, Nat. Hazards Earth Syst. Sci., 3, 725–732, https://doi.org/10.5194/nhess-3-725-2003, 2003.

Kodama, C., Stevens, B., Mauritsen, T., Seiki, T., & Satoh, M. (2019). A New Perspective for Future Precipitation Change from Intense Extratropical Cyclones. Geophysical Research Letters, 46, 12435–12444. https://doi.org/10.1029/2019GL084001

Lockwood, J. F., N. Dunstone, L. Hermanson, G. R. Saville, A. A. Scaife, D. Smith, and H. E. Thornton, 2023: A Decadal Climate Service for Insurance: Skillful Multiyear Predictions of North Atlantic Hurricane Activity and U.S. Hurricane Damage. J. Appl. Meteor. Climatol., 62, 1151–1163, https://doi.org/10.1175/JAMC-D-22-0147.1.

Lodise, J.; Merrifield, S.; Collins, C.; Behrens, J.; Terrill, E. Performance of ERA5 wind speed and significant wave height within Extratropical cyclones using collocated satellite radar altimeter measurements. *Coast. Eng. J.* **2024**, *66*, 89–114.

Martínez-Asensio, A., Tsimplis, M.N., Marcos, M., Feng, X., Gomis, D., Jordà, G. and Josey, S.A. (2016), Response of the North Atlantic wave climate to atmospheric modes of variability. Int. J. Climatol., 36: 1210-1225. https://doi.org/10.1002/joc.4415

Martius, O., S. Pfahl, and C. Chevalier (2016), A global quantification of compound precipitation and wind extremes, *Geophys. Res. Lett.*, 43, 7709–7717, doi:10.1002/2016GL070017.

Matthews, T., Murphy, C., Wilby, R. *et al.* Stormiest winter on record for Ireland and UK. *Nature Clim Change* **4**, 738–740 (2014). https://doi.org/10.1038/nclimate2336

Minola, L., Zhang, F., Azorin-Molina, C. *et al.* Near-surface mean and gust wind speeds in ERA5 across Sweden: towards an improved gust parametrization. *Clim Dyn* **55**, 887–907 (2020). https://doi.org/10.1007/s00382-020-05302-6

Moemken, J., Alifdini, I., Ramos, A. M., Georgiadis, A., Brocklehurst, A., Braun, L., and Pinto, J. G.: Insurance loss model vs. meteorological loss index – how comparable are their loss estimates for European windstorms?, Nat. Hazards Earth Syst. Sci., 24, 3445–3460, https://doi.org/10.5194/nhess-24-3445-2024, 2024.

Owen LE, Catto JL, Stephenson DB, Dunst one NJ. Compound precipitation and wind extremes over Europe and their relationship to extratropical cyclones. Weather Clim Extremes (2021) 33:100342. doi: 10.1016/j.wace.2021.100342

Pinto, J.G., Zacharias, S., Fink, A.H. et al. Factors contributing to the development of extreme North Atlantic cyclones and their relationship with the NAO. Clim Dyn 32, 711–737 (2009). https://doi.org/10.1007/s00382-008-0396-4

Priestley, M. D. K., & Catto, J. L. (2022). Improved representation of extratropical cyclone structure in HighResMIP models. Geophysical Research Letters, 49, e2021GL096708. https://doi.org/10.1029/2021GL096708

Ramon J, Lledó L, Torralba V, Soret A, Doblas-Reyes FJ. What global reanalysis best represents near-surface winds?. Q J R Meteorol Soc. 2019; 145: 3236–3251. https://doi.org/10.1002/qj.3616

Scaife, A. A., C. K. Folland, L. V. Alexander, A. Moberg, and J. R. Knight, 2008: European Climate Extremes and the North Atlantic Oscillation. J. Climate, 21, 72–83, https://doi.org/10.1175/2007JCLI1631.1.

Scaife, A. A., et al. (2014), Skillful long-range prediction of European and North American winters, *Geophys. Res. Lett.*, 41, 2514–2519, doi:10.1002/2014GL059637.

Seneviratne, S.I., X. Zhang, M. Adnan, W. Badi, C. Dereczynski, A. Di Luca, S. Ghosh, I. Iskandar, J. Kossin, S. Lewis, F. Otto, I. Pinto, M. Satoh, S.M. Vicente-Serrano, M. Wehner, and B. Zhou, 2021: Weather and Climate Extreme Events in a Changing Climate. In Climate Change 2021: The Physical Science Basis. Contribution of Working Group I to the Sixth Assessment Report of the Intergovernmental Panel on Climate Change[Masson-Delmotte, V., P. Zhai, A. Pirani, S.L. Connors, C. Péan, S. Berger, N. Caud, Y. Chen, L. Goldfarb, M.I. Gomis, M. Huang, K. Leitzell, E. Lonnoy, J.B.R. Matthews, T.K. Maycock, T. Waterfield, O. Yelekçi, R. Yu, and B. Zhou (eds.)]. Cambridge University Press, Cambridge, United Kingdom and New York, NY, USA, pp. 1513–1766, doi: 10.1017/9781009157896.013.

Stone, D.A. A hierarchical collection of political/economic regions for analysis of climate extremes. Climatic Change 155, 639–656 (2019). https://doi.org/10.1007/s10584-019-02479-6

Thornton, H. E., Smith, D. M., Scaife, A. A., & Dunstone, N. J. (2023). Seasonal predictability of the East Atlantic Pattern in late autumn and early winter. *Geophysical Research Letters*, 50, e2022GL100712. https://doi.org/10.1029/2022GL100712

Acknowledgements

ACM, CMM and JP acknowledge funding from the H2020 CONSTRAIN project (grant agreement no. 820829). ACM acknowledges funding from the NERC Stratclust project (NE/X011933/1). JP was funded by the EPSRC Centre for Doctoral Training in Fluid Dynamics at Leeds (EP/S022732/1).

Author contributions

ACM conceived the study. MDKP produced the storm tracks and cyclone footprints. CMM analysed the data and produced figures. JP produced figures. ACM wrote the paper with contributions from all authors.

Data availability statement

The ERA5 data is available for the Copernicus Climate Data Store. The TRACK algorithm is available on request from Kevin Hodges at the University of Reading.

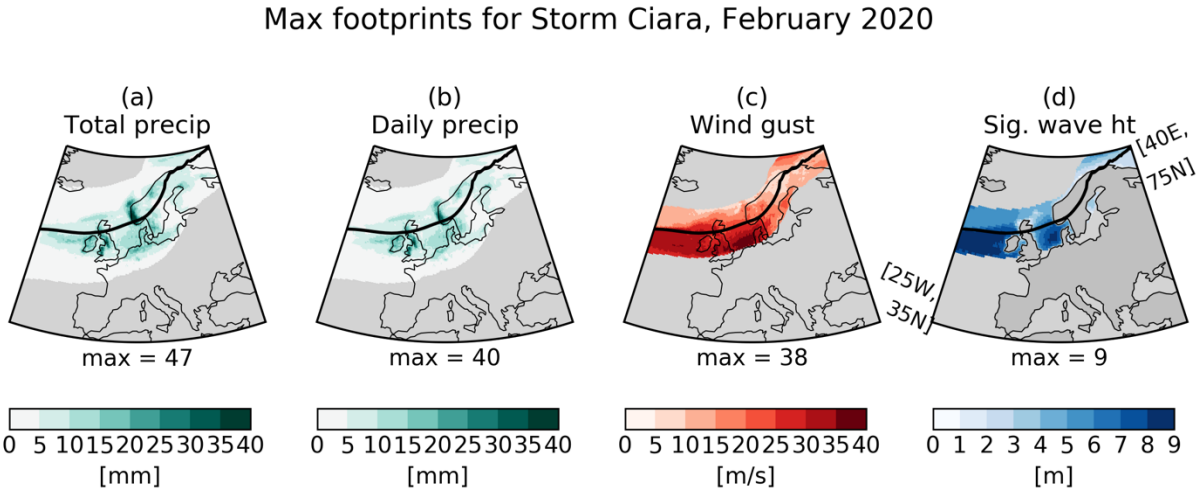

Figure 1: An example ETC footprint lifecycle for the four measures of ETC hazards (a) Cumulative precipitation over the cyclone lifetime, (b) maximum daily precipitation over lifetime, (b) local maximum 10m wind gust over lifetime, and (c) local maximum significant wave height over lifetime for Storm Ciara in February 2020 (track shown by black line).

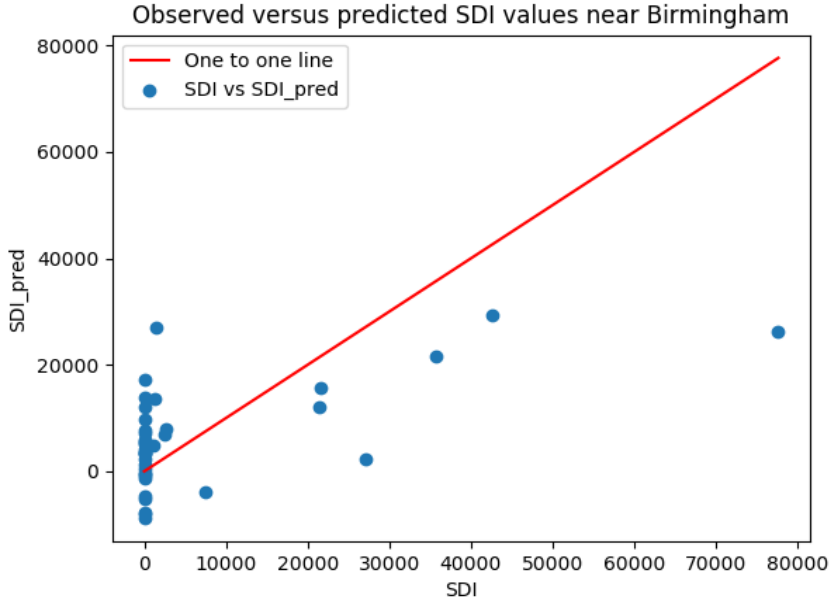

Figure 2: Winter cumulative SDI (x-axis) vs. predicted SDI based on the multiple linear regression between SDI and the PC1 and PC2 timeseries (y-axis) at grid box (1.875°W, 52.5°N). Red line shows 1:1 line. Note some of the predicted SDI values are negative when it is bounded at 0.

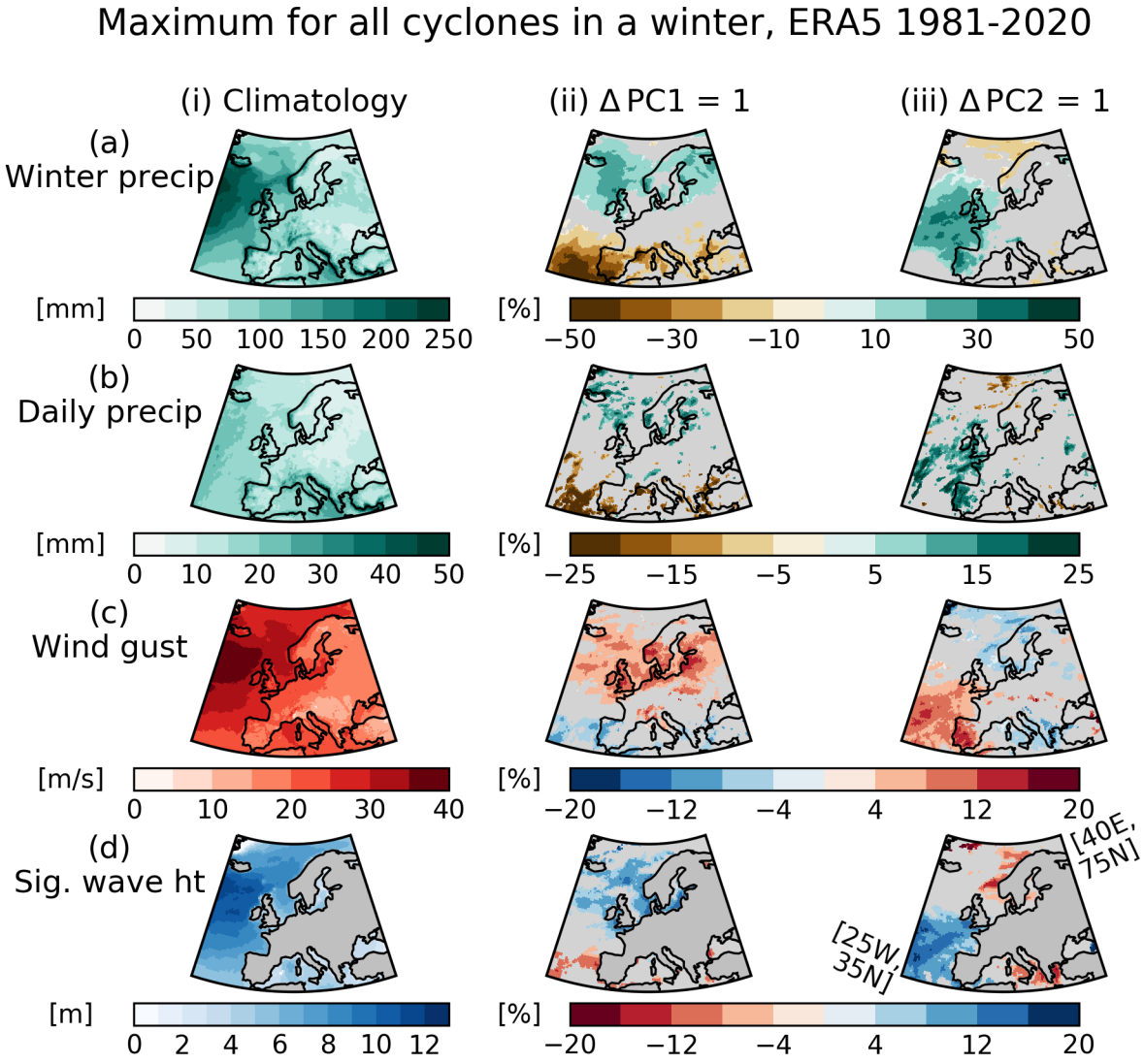

Figure 3: Maximum winter ETC hazards for (a) winter total precipitation [mm], (b) winter daily maximum precipitation [mm], (c) 10m wind gust [m/s] and (d) maximum significant wave height [m] for (left column) climatology, (middle column) regression onto PC1 and (right column) regression onto PC2 shown as percentage anomalies from the climatology. Note significant wave height is only defined over ocean points. Grey areas in middle and right columns denote regions where the regression slope is not significantly different from zero at the 95% confidence level.

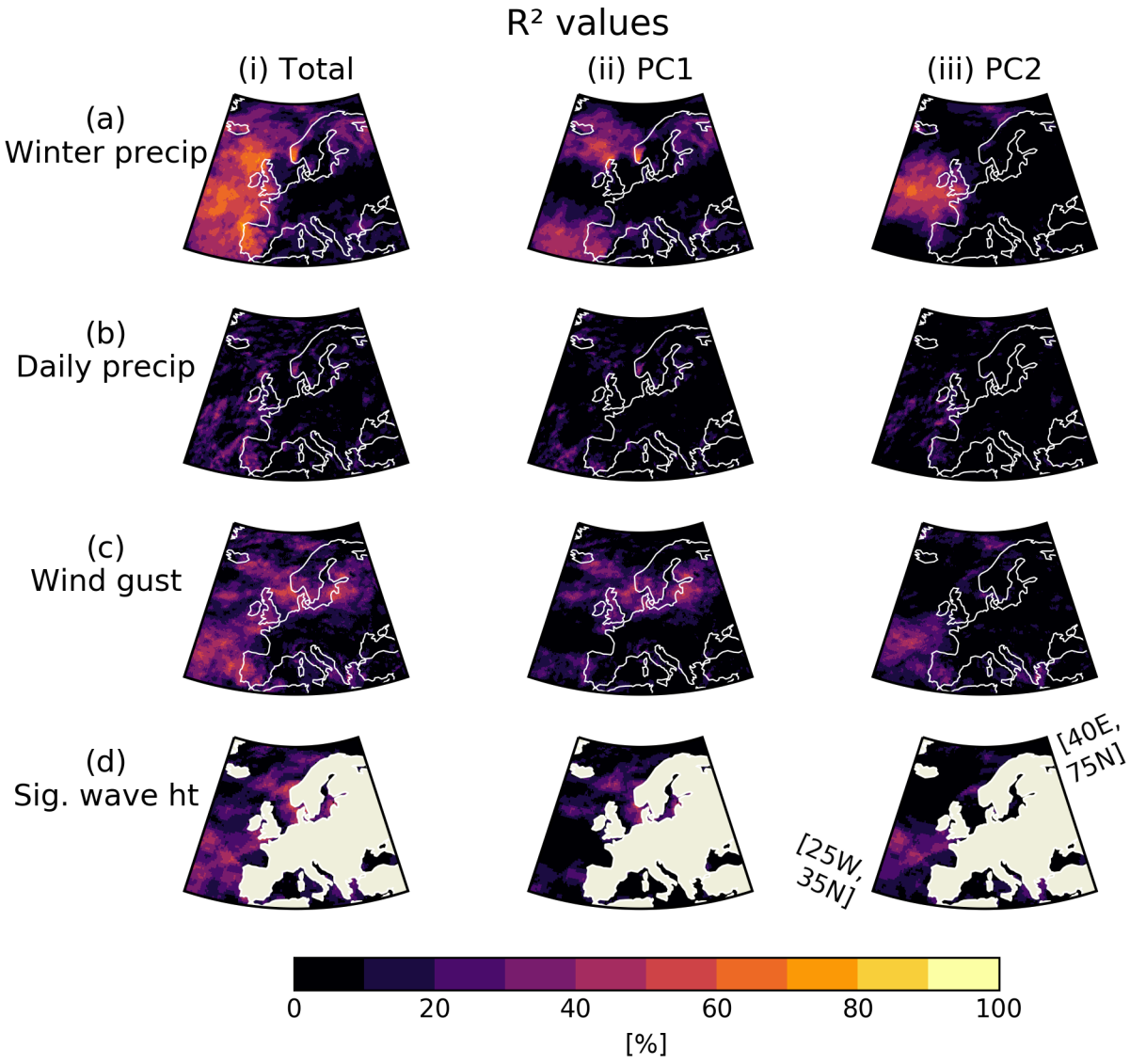

Figure 4: R^2 values [%] for the linear regression of ETC winter hazards (a) winter total precipitation, (b) winter daily maximum precipitation, (c) maximum 10m wind gust and (d) maximum significant wave height for (left) PC1+PC2, (middle) PC1 and (right) PC2.

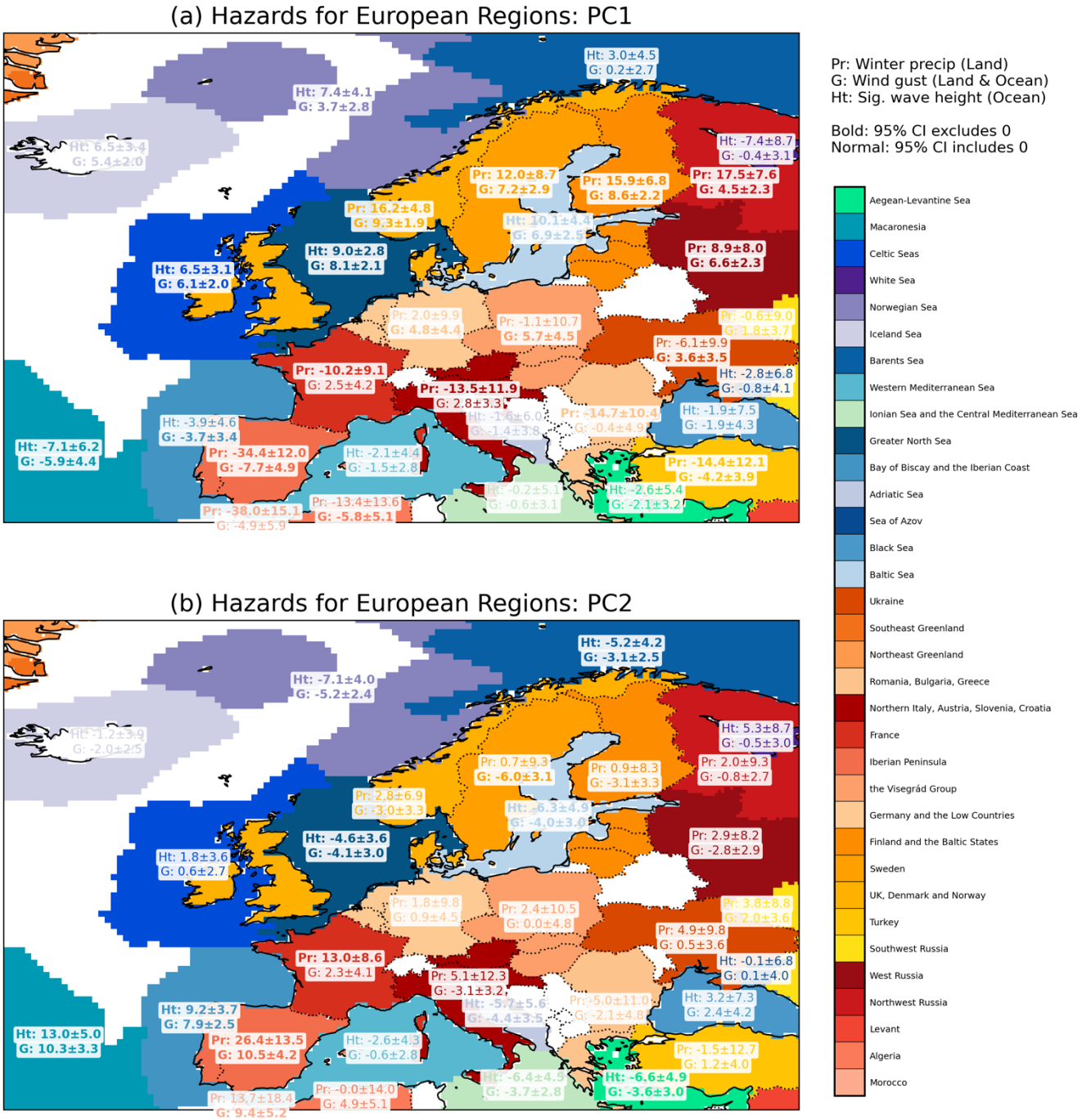

Figure 5: Regional percentage anomalies in winter ETC hazards for land and sea regions as labelled associated with (a) PC1 and (b) PC2. Hazards are winter total precipitation (Pr) and winter maximum wind gust (G) for land regions (red/yellow palette) and significant wave height for regional sea areas (Ht; green/purple/blue palette). Labels denote % anomalies

associated with 1 sigma of the PC index with errors representing 1 standard error (SE). Bold text denotes values which do not overlap zero within ±1 SE.

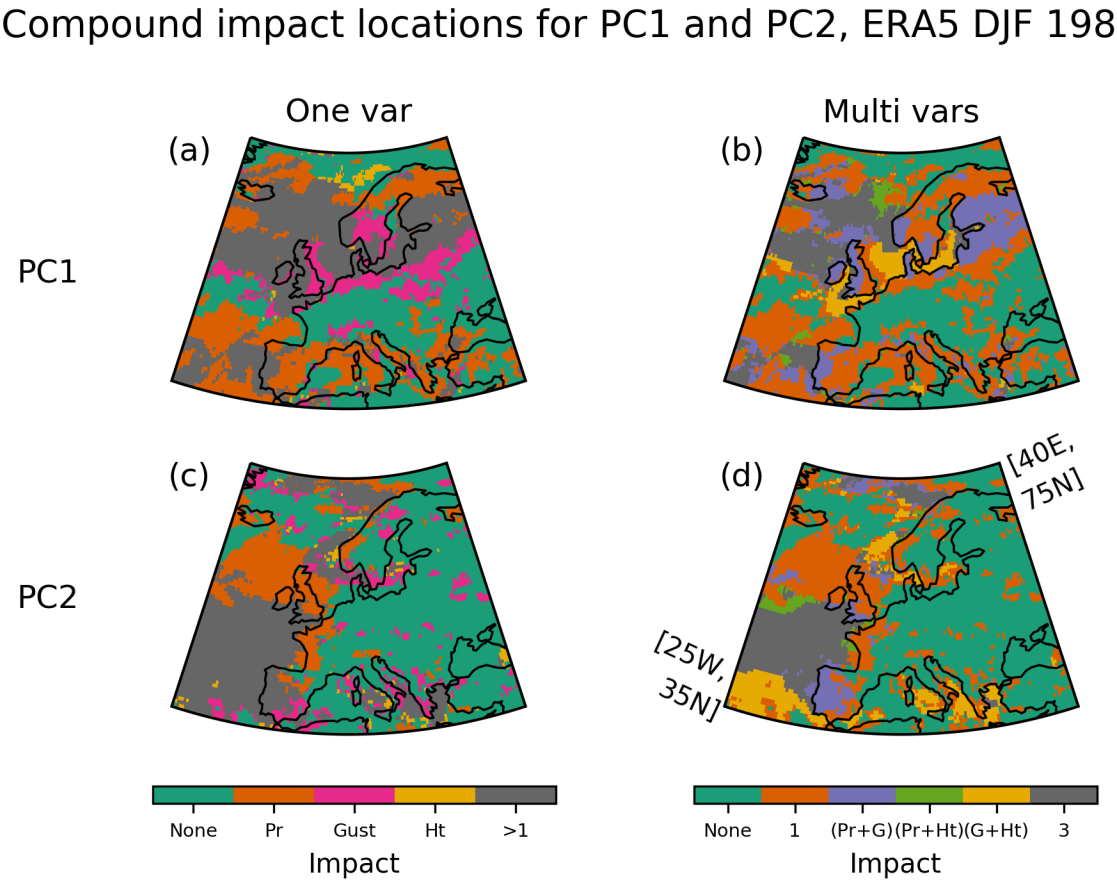

Figure 6: Compound ETC hazards for (a) PC1 and (b) PC2. (Left) Regions affected by single hazards (Winter total precipitation, Pr, orange; Maximum 10m wind gust, Gust, Pink; Maximum significant wave height, Ht, yellow), no hazard (green) or >1 hazard (grey); (right) regions affected by compound hazards as labelled. Note the hazards may not occur on the same day.

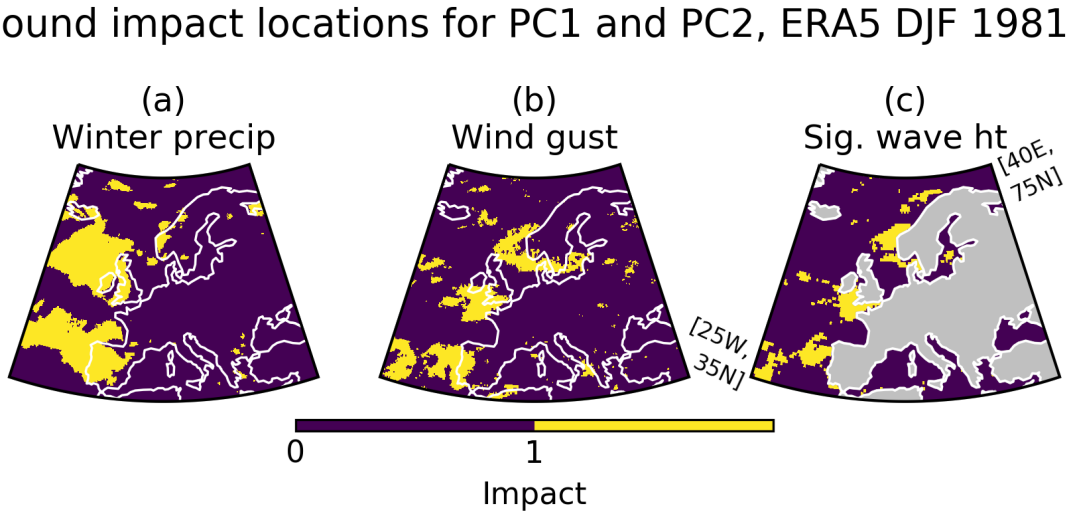

Figure 7: Coincident spatial signals for combined PC1 and PC2 in individual ETC hazards (a) winter maximum daily precipitation, (b) winter maximum 10m wind gust and (c) winter maximum significant wave height. Yellow denotes compound impact locations between PC1 and PC2 for each hazard, purple denotes no effect or no compound effect.

605

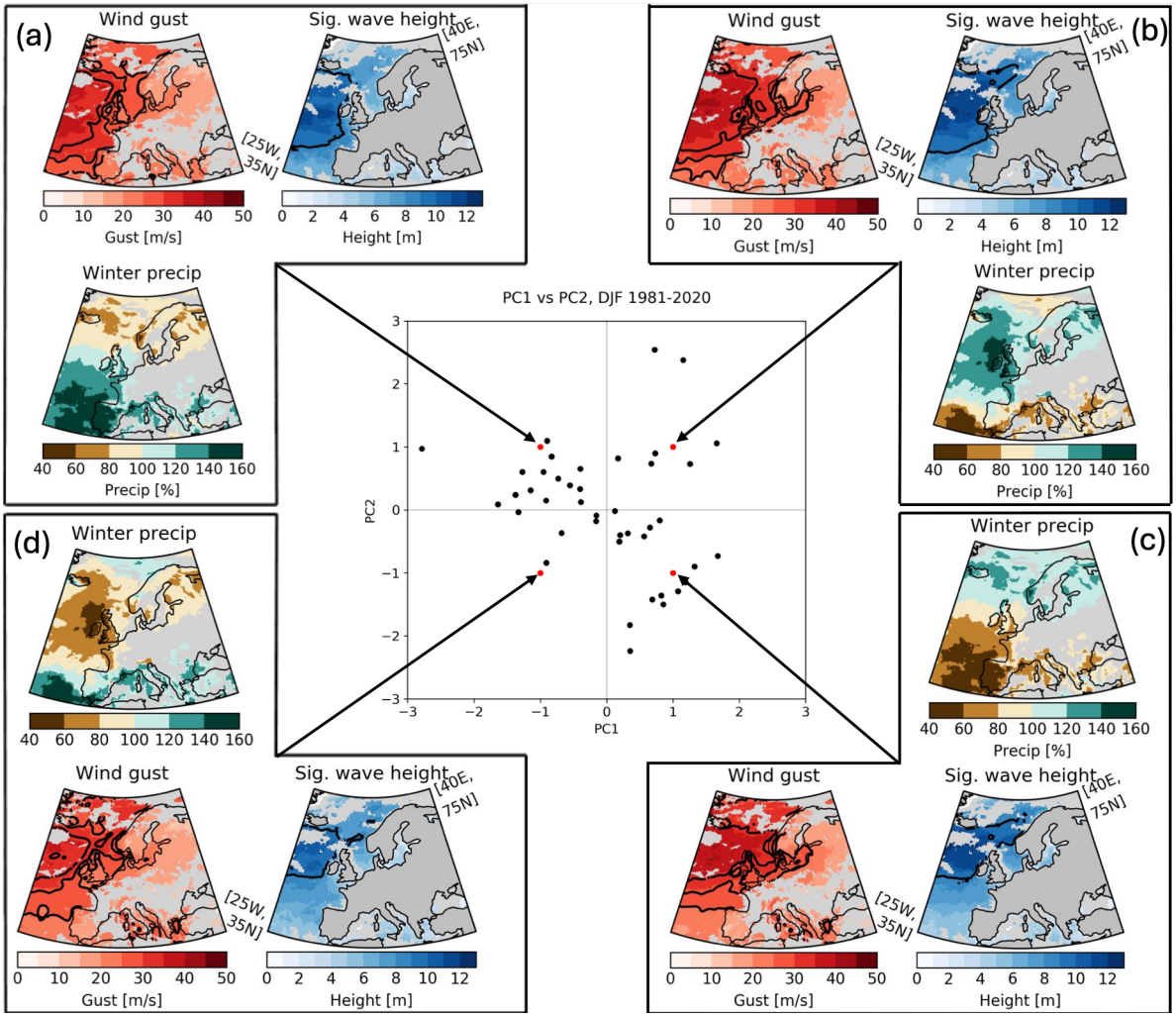

610

Figure 8: Absolute values of winter maximum 10m wind gust (m/s) and maximum significant wave height (m), with maximum daily precipitation shown as a percentage of climatology (%) predicted by the linear regression model for ±1σ combinations of PC1/PC2 indices (four combinations shown by red dots in middle panel). Black contours in gust panels show 25 m/s (severe gale), 29 m/s (violent storm), 33 m/s (hurricane strength) thresholds based on the Beaufort scale. Black contours in significant
615 wave height panels show 9 m (very high) and 14 m (phenomenal) based on the Douglas Sea Scale. Black points in middle panel show historical winter PC1/PC2 indices from ERA5.